JOC The Journal of Organic Chemistry

Article

pubs.acs.org/joc

Synthesis, Photophysical and Photochemical Properties of Photoacid Generators Based on *N*-Hydroxyanthracene-1,9-dicarboxyimide and Their Application toward Modification of Silicon Surfaces

Mohammed Ikbal, Rakesh Banerjee, Sanghamitra Atta, Dibakar Dhara,* Anakuthil Anoop,* and N. D. Pradeep Singh*

Department of Chemistry, Indian Institute of Technology Kharagpur, Kharagpur-721302, India

Supporting Information

ABSTRACT: We have introduced a series of nonionic photoacid generators (PAGs) for carboxylic and sulfonic acids based on *N*-hydroxyanthracene-1,9-dicarboxyimide (HADI). The newly synthesized PAGs exhibited positive solvachromatic emission (λ_{max}(hexane) 461 nm, λ_{max}(ethanol) 505 nm) as a function of solvent polarity. Irradiation of PAGs in acetonitrile (ACN) using UV light above 410 nm resulted in the cleavage of weak N−O bonds, leading to the generation of carboxylic and sulfonic acids in good quantum and chemical yields. Mechanism for the homolytic N−O bond cleavage for acid generation was supported by time-dependent density functional theory (TD-DFT) calculations. More importantly, using the PAG monomer *N*-(*p*-vinylbenzenesulfonyloxy)anthracene-1,9-dicarboxyimide (VBSADI), we have synthesized *N*-(*p*-vinylbenzenesulfonyloxy)-anthracene-1,9-dicarboxyimide−methyl methacrylate (VBSADI-MMA) and *N*-(*p*-vinylbenzenesulfonyloxy)anthracene-1,9-dicarboxyimide−ethyl acrylate (VBSADI-EA) copolymer through atom transfer radical polymerization (ATRP). Finally, we have also developed photoresponsive organosilicon surfaces using the aforementioned polymers.

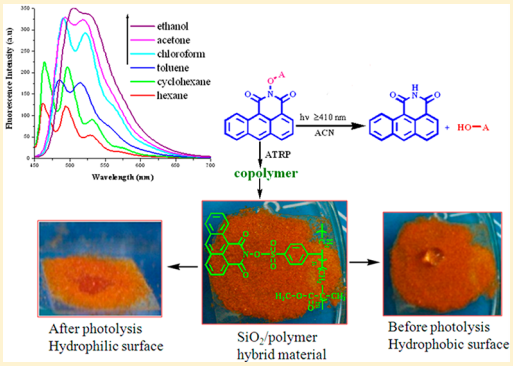

INTRODUCTION

Over the past few decades, photoacid generators (PAGs) have gained enormous interest, due to their immense applications in the microlithographic industry.[1] PAGs are the key material used in the field of photoresists for semiconductor fabrication.[2] Photoirradiation of a polymer film containing a PAG results in generation of acid, which catalyzes certain important chemical transformations within the polymer film such as deprotection of functional groups, initiation of polymerization, and cross-linking processes.[3,4] These processes either make the polymer more soluble in the developing solvent, resulting in positive resists, or less soluble, generating negative resists. Generally, two types of PAGs are known: ionic[5] and nonionic[6] types. A large number of onium salts based on ionic PAGs such as aryldiazonium, diaryliodonium, triarylsulfonium, and triarylphosphonium are known, and their photochemistry has been investigated in detail.[7] On the other hand, among nonionic PAGs, iminosulfonates,[8] *N*-hydroxyimide sulfonates,[7] tris(methylsulfonyloxy)benzene,[7] and 1-(sulfonoxy)-2-quinolone[9] are known to generate sulfonic acids through homolytic N−O bond cleavage. Due to the limited solubility of the onium salts in common organic solvents, nonionic PAGs have gained much attention over the ionic types.[10]

Recently, the use of PAG-containing polymers for the development of smart photoresponsive surfaces[11] and inorganic/polymer hybrid materials,[12] which can change their surface wettability in the presence of external light, has emerged as an exciting topic in surface science and materials chemistry. Numerous research groups are working on the development of inorganic/polymer hybrid materials, since inorganic and organic materials have complementary properties. Especially, inorganic materials have good mechanical and thermal stability, while organic compounds can provide flexibility, hydrophobicity, and versatility for further functionalization.[13] To date, several techniques[14] have been attempted to combine these two materials to create new kinds of materials which will possess better thermal, chemical, and mechanical properties. In particular, the modification of silica surfaces via the formation of a SiO_2/polymer hybrid material usually known as organosilica[15] has long been studied and utilized in many fields of chemistry, mainly in chromatography[16] and catalysis.[17] More recently, organosilica appears as a key topic in areas such as polymer nanocompounds[18] and the development of hydrophobic[19] and superhydrophobic materials.[20]

In recent years, our research interest in the development of PAGs[9,21] based on N−O bond cleavage chemistry has drawn our attention toward the well-established PAGs sulfonyloxyphthalimide[22] (PIT) and sulfonyloxy-1,8-naphthalimide[23] (NIT), as they have a weak N−O bond which can be easily cleaved

Received: July 9, 2012
Published: November 11, 2012

ACS Publications © 2012 American Chemical Society

Scheme 1. Synthesis of HADI-Based PAGs 3a−e and 4a−e

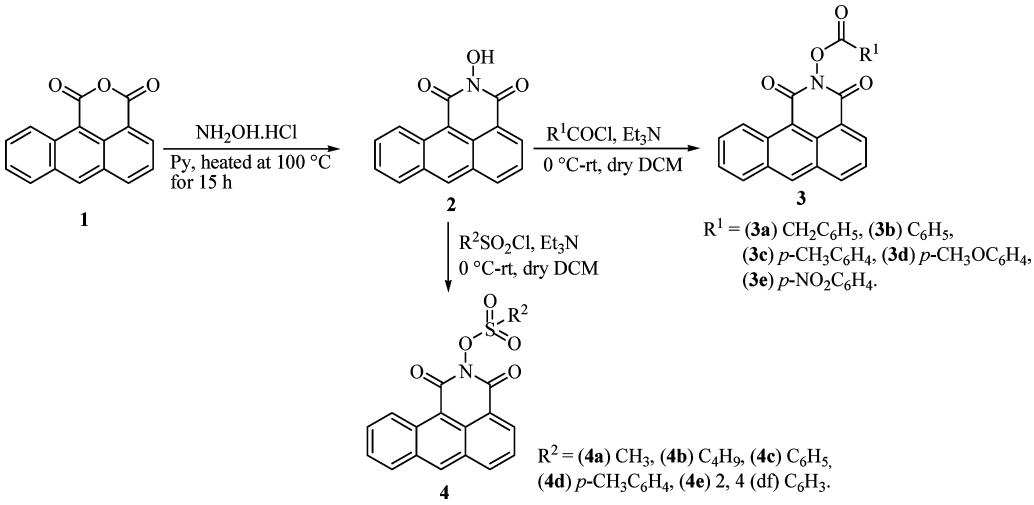

Table 1. Synthetic Yields, UV/Vis, and Fluorescence Data of PAGs 3a−e and 4a−e

			photophysical data in EtOH				
			UV/vis		fluorescence		
PAG	acid chloride	synthetic yield (%)[a]	λ_{max} (nm)[b]	log ε[c]	λ_{max} (nm)[d]	Stokes shift (nm)[e]	Φ_f[f]
3a	$C_6H_5CH_2COCl$	80	438	3.92	523	86	0.45
3b	C_6H_5COCl	82	438	3.87	521	83	0.43
3c	p-$CH_3C_6H_4COCl$	80	437	3.86	522	85	0.41
3d	p-$CH_3OC_6H_4COCl$	79	437	3.85	522	85	0.42
3e	p-$NO_2C_6H_4COCl$	75	437	3.82	524	88	0.38
4a	CH_3SO_2Cl	82	438	4.01	524	85	0.60
4b	$C_4H_9SO_2Cl$	80	439	4.05	523	83	0.61
4c	$C_6H_5SO_2Cl$	75	437	3.93	523	85	0.56
4d	p-$CH_3C_6H_4SO_2Cl$	80	437	3.96	524	86	0.59
4e	2, 4 (df) $C_6H_3SO_2Cl$	79	438	3.97	522	84	0.58
	anthracene		356		400		0.27

[a]Based on isolated yield. [b]Maximum absorption wavelength. [c]Molar absorption coefficient at the maximum absorption wavelength. [d]Maximum emission wavelength. [e]Difference between maximum absorption wavelength and maximum emission wavelength. [f]Fluorescence quantum yield (error limit within ±5%).

upon UV irradiation. Among these, 1,8-naphthalimide-based photoacid generators bearing different kinds of substituents exhibited good fluorescence properties.[23] Especially, the fluorescence nature and acid generation ability of NIT prompted us to design a new fluorescent PAG based on the NIT skeleton which can be used both for generation of carboxylic and sulfonic acids by irradiating with light above 410 nm and for the development of photoresposive organosilicon surfaces.

Hence, herein we report new fluorescent PAGs based on *N*-hydroxyanthracene-1,9-dicarboxyimide (HADI) for carboxylic and sulfonic acids. In the present study, we describe the synthesis, characterization, and photophysical properties of the anthracene-1,9-dicarboxyimide-based PAGs. We examine the acid generation ability of PAGs by irradiating with light above 410 nm. The mechanism of photochemical N−O bond cleavage is analyzed using time-dependent density functional theory. The polymers VBSADI-MMA and VBSADI-EA were synthesized through the ATRP process using a PAG monomer (VBSADI). Moreover, we also discuss the surface modification of silica (60−120 mesh) by using VBSADI-MMA polymer and investigate the photoresponsive behavior of the modified silicon surface[24] in terms of controlled wettability.

RESULTS AND DISCUSSION

1. HADI-Based PAGs for Carboxylic and Sulfonic Acids: Synthesis of PAGs 3a−e and 4a−e. We have synthesized HADI based PAGs **3a−e** and **4a−e** as outlined in Scheme 1. Anthracene-1,9-dicarboxylic anhydride (**1**) was prepared by following the literature procedure.[25] Condensation of **1** with hydroxylamine hydrochloride in dry pyridine at 100 °C yielded *N*-hydroxyanthracene-1,9-dicarboxyimide[26] (**2**). Treatment of **2** with various carboxylic and sulfonyl chlorides in the presence of triethylamine in dry DCM at 0 °C resulted in the formation of PAGs **3a−e** and **4a−e** in moderate to good yields (Table 1). All the PAGs were characterized by ^{1}H and ^{13}C NMR, FTIR, and mass spectral analysis.

2. Photophysical Properties of HADI-Based PAGs. *2.1. Absorption and Emission Properties of PAGs **3a−e** and **4a−e**.* The UV/vis absorption spectra of degassed 1.5×10^{-5} M solution of PAGs **3a−e** in ethanol (EtOH) have been recorded, and the results are tabulated in Table 1. All the PAGs exhibited similar kinds of absorption (Figure 1) and emission (Figure F1, see supporting information page-S8) behaviour, indicating that substituents on the aromatic ring of the carboxyl moiety have no significant effect on the photophysical properties of HADI. The absorption wavelengths of all the

dx.doi.org/10.1021/jo301367y | J. Org. Chem. 2012, 77, 10557−10567

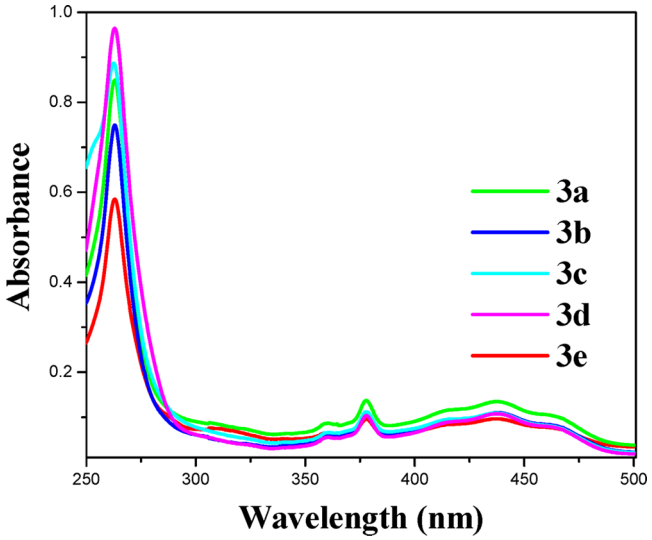

Figure 1. UV/vis absorption spectra of PAGs **3a**–**e** in EtOH (1.5×10^{-5} M).

PAGs are significantly red-shifted by ~85 nm in comparison to the parent anthracene. This is due to the efficient π conjugation and donor–acceptor interaction between the anthracene moiety and the dicarboxylic imide group.[27] Figure 2 shows

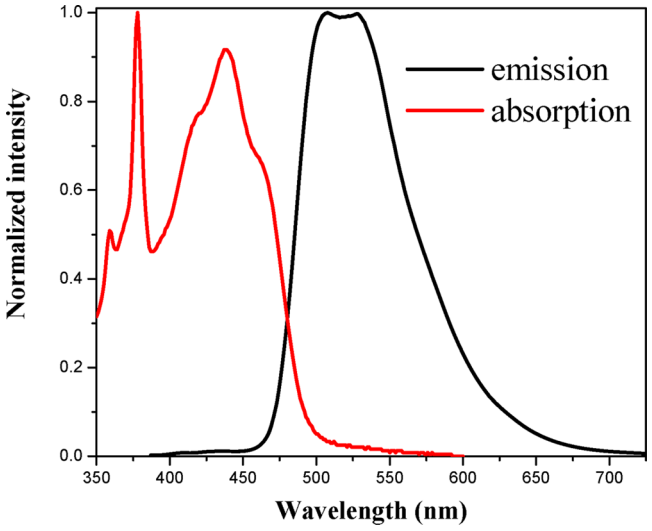

Figure 2. Normalized UV/vis absorption spectrum (red line) and emission spectrum (black line) of PAG **3c** in EtOH (1.5×10^{-5} M).

the normalized absorption and the emission spectra of PAG **3c** in ethanol. The absorption spectrum of **3c** has an intense band centered at 437 nm, while in the emission spectrum the emission maximum was red-shifted to about 524 nm. Similar photophysical properties were also noted for PAGs of sulfonic acids (**4a**–**e**) (see the Supporting Information, Figure F2a,b, p S14).

2.2. Solvent-Dependent Fluorescence Properties of PAGs. The excited-state properties of the PAGs were investigated by emission spectroscopy. These synthesized PAGs showed positive solvachromatic emission as a function of solvent polarity. As a representative example, the emission spectra of **3a** in solvents of increasing polarity are shown in Figure 3, which indicates a strong solvent-dependent fluorescence. As the solvent polarity increases (hexane to ethanol), a bathochromic

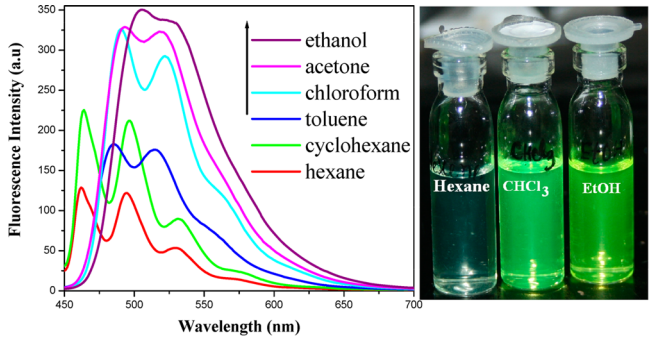

Figure 3. Fluorescence spectra of **3a** (0.5×10^{-5} M) in solvents of different polarity and hydrogen-bonding capabilities.

shift along with an increase in fluorescence intensity for **3a** was noticed and the emission maximum was found to shift from 461 to 505 nm. Moreover, the fluorescence quantum yield (Φ_f) of **3a** was also found to increase from 0.39 to 0.52 as we changed the solvent from hexane to acetone (Table 2). The

Table 2. Photophysical Data of PAG 3a in Different Solvents

solvent	ε(25 °C)	λ_{max}(abs) (nm)[a]	log ε[b]	λ_{max}(em) (nm)[c]	Φ_f[d]
hexane	1.882	429	3.50	461	0.39
cyclohexane	2.015	431	3.75	463	0.50
toluene	2.379	437	3.66	484	0.51
chloroform	4.806	438	3.38	489	0.48
acetone	20.70	437	3.37	493	0.52
ethanol	24.30	438	3.92	505	0.45

[a]Maximum absorption wavelength. [b]Molar absorption coefficient at the maximum absorption wavelength. [c]Maximum emission wavelength. [d]Fluorescence quantum yield (error limit within ±5%), calculated using quinine sulfate as a standard (Φ_f = 0.546[30]) in EtOH.

solvent effect observed above is due to a large increase in the dipole moment of the PAG on excitation, followed by solvent relaxation. Further, we also noticed a bathochromic shift as we moved from chloroform to a hydrogen-bonding polar solvent (ethanol), indicating an intermolecular hydrogen bond between unshared electron pairs on the carbonyl oxygen of PAG with ethanol. The above solvent effect was also noted in the case of N-substituted benzoperylene monoimides.[28,29]

3. Photoacid Generation and Quantum Yield Measurement for PAGs 3a–e and 4a–e. To demonstrate the acid generation ability of newly synthesized PAGs, we irradiated PAGs **3a**–**e** and **4a**–**e** (2.0×10^{-4} M) individually, in N_2-saturated acetonitrile solution using a 125 W medium-pressure Hg lamp as the visible light source (≥410 nm) and a 1 M $NaNO_2$ solution as the UV cutoff filter. We noted that all the PAGs generated corresponding carboxylic (**6a**–**e**) and sulfonic acids (**7a**–**e**) in good chemical yields (75–85%) along with the major photoproduct anthracene-1,9-dicarboxyimide (**5**) (Scheme 2). Quantum yields for the generation of acids by the corresponding PAGs were calculated and found to be within the range of 0.26–0.35 (Φ_p) (Table 3), using potassium ferrioxalate as an actinometer.[31]

As a representative example, we have presented the UV/vis and fluorescence spectral change of PAG **4d** at regular intervals of irradiation time (see the Supporting Information, Figure F3a,b, p S14).

dx.doi.org/10.1021/jo301367y | J. Org. Chem. 2012, 77, 10557–10567

Scheme 2. Photogeneration of Carboxylic and Sulfonic Acids by PAGs 3a−e and 4a−e

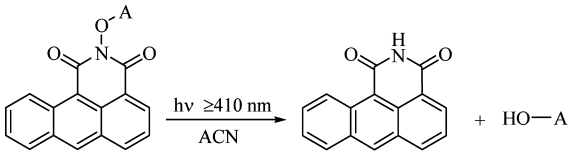

3a-e or **4a-e** **5** **6a-e** or **7a-e**

Table 3. Photolytic Data of PAGs 3a−e and 4a−e on Irradiation by Visible Light (≥410 nm) in Acetonitrile

		photolytic data of PAGs		
PAGs	carboxylic (**6a−e**) and sulfonic acids (**7a−e**)	time of photolysis (min)[a]	acid generated (%)[b]	quantum yield (Φ_p)[c]
3a	$C_6H_5CH_2CO_2H$	255	80	0.29
3b	$C_6H_5CO_2H$	252	82	0.30
3c	p-$CH_3C_6H_4CO_2H$	240	80	0.31
3d	p-$CH_3C_6H_4CO_2H$	230	85	0.34
3e	p-$NO_2C_6H_4CO_2H$	265	75	0.26
4a	CH_3SO_3H	240	82	0.32
4b	$C_4H_9SO_3H$	235	85	0.34
4c	$C_6H_5SO_3H$	225	80	0.33
4d	p-$CH_3C_6H_4CO_2H$	220	83	0.35
4e	2,4-(df)$C_6H_3SO_3H$	230	80	0.32

[a]Time of photolysis. [b]Percent of carboxylic acid generated as determined by HPLC and of sulfonic acid as determined by ^{1}H NMR. [c]Photochemical quantum yield for the generation of carboxylic and sulfonic acids (error limit within ±5%).

4. Possible Mechanism for the Photogeneration of Carboxylic Acids 6a−e and Sulfonic Acids 7a−e. On the basis of literature studies reported for the photodecomposition of *N*-oxyimidosulfonate[32] and *N*-tosyloxyphthalimide,[22] we proposed a possible mechanism for the photogeneration of carboxylic and sulfonic acids, as shown in Scheme 3. After initial photoexcitation of the PAG to its singlet excited state, it undergoes N−O bond cleavage to generate a radical pair. The radical pair generated above in polar solvent undergoes solvent cage escape following hydrogen abstraction from the solvent to produce the corresponding acid (carboxylic acids **6a−e** or sulfonic acids **7a−e**) and anthracene-1,9-dicarboxyimide (**5**).

*4.1. Computational Study of N−O Bond Cleavage for PAG **3b**.* In support of the above mechanistic proposal, we have carried out time-dependent density functional theory (TD-DFT) calculations (see Computational Methods below for details), considering the dissociation of PAG **3b** as a representative example. We have considered two conformational possibilities of **3b**, resulting from the relative orientation of the phenyl group with respect to the anthracenyl moiety, characterized by the torsion angle N−O−C(O)−C(Ph), either 0 or 180°. The former conformation **A**, where the phenyl group is placed above the anthracenyl moiety, is found to be 5.32 kcal/mol higher in energy in comparison to the latter conformation (**B**), in which the phenyl group stays away from the anthracenyl moiety (see the Supporting Information p S17 for geometries). Hence, conformation **B** is considered for detailed analysis at the PBE/def2-SVP level of theory. TD-DFT calculations revealed that thermal dissociation from the ground state (S0) is much more endothermic for the heterolytic dissociation to yield ions (183.23 kcal/mol) in comparison to homolytic cleavage to form a separate radical pair (66.38 kcal/mol). The effect of solvent is introduced to account for the stabilization of ions in the solvent media, using the continuum solvation model (COSMO with $\varepsilon' = 35.688$). In the solvent media, the dissociation energies for heterolytic and homolytic cleavage were reduced to 82.02 and 60.32 kcal/mol, respectively. The dissociation energy for homolytic dissociation from the S1 state is found to be 20.75 kcal/mol. The inclusion of solvent effects reduced the dissociation energy to −12.58 kcal/mol (exothermic).

Vertical excitation energy for the lowest singlet ($\pi-\pi^*$) excitation was computed using TD-DFT calculations with five different functionals at the geometry optimized at the PBE/def2-SVP level. The vertical excitation energies are 514 nm (PBE/def2-SVP), 458 nm (B3LYP-D/6-31+G*), 407 nm (CAM-B3LYP/6-31+G*), 444 nm (PBE0/6-31+G*), and 471 nm (TPSSh/6-31+G*). Considering the accuracy of TD-DFT methods, these values are in reasonable agreement with a λ_{max} value of 438 nm for **3b**. We have further optimized the excited S1 state using PBE/def2-SVP. The adiabatic excitation energy is 45.63 kcal/mol (in comparison to the vertical excitation energy of 55.63 kcal/mol). The computed Stokes shift is 71 nm, which is in good agreement with the experimental value of 83 nm.

The potential energy surface (PES) for dissociation through the S1 state was computed to analyze the dissociation process and to locate the transition state. The PES was calculated with a relaxed surface scan, where the N−O bond distance was restrained along the reaction coordinate and all other degrees of freedom were optimized. Similarly, the ground state PES was also computed for comparison. In the ground state the energy continuously increases, while in the S1 state the energy increases up to 1.712 Å and decreases on increasing the distance further (Figure 4).

The geometry with the highest S1 state energy was used as the starting estimate for transition state optimization. At the TS geometry, the N−O bond is bent out of the plane containing anthracene. The N−O distance is 1.717 Å. The activation energy ($\Delta E^{\ddagger}$) for the N−O bond dissociation in the S1 state at

Scheme 3. Possible Mechanism for the Photogeneration of Carboxylic and Sulfonic Acids

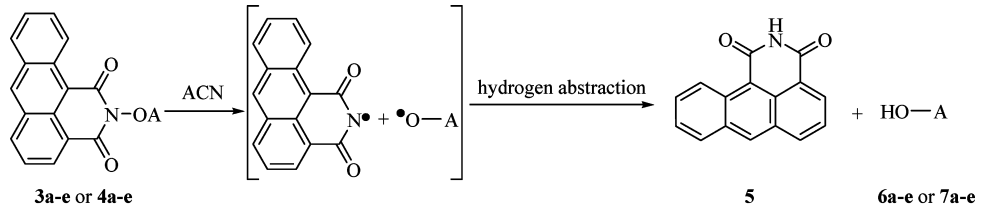

3a-e or **4a-e** **5** **6a-e** or **7a-e**

A = -COR[1] or -SO_2R^2

dx.doi.org/10.1021/jo301367y | J. Org. Chem. 2012, 77, 10557−10567

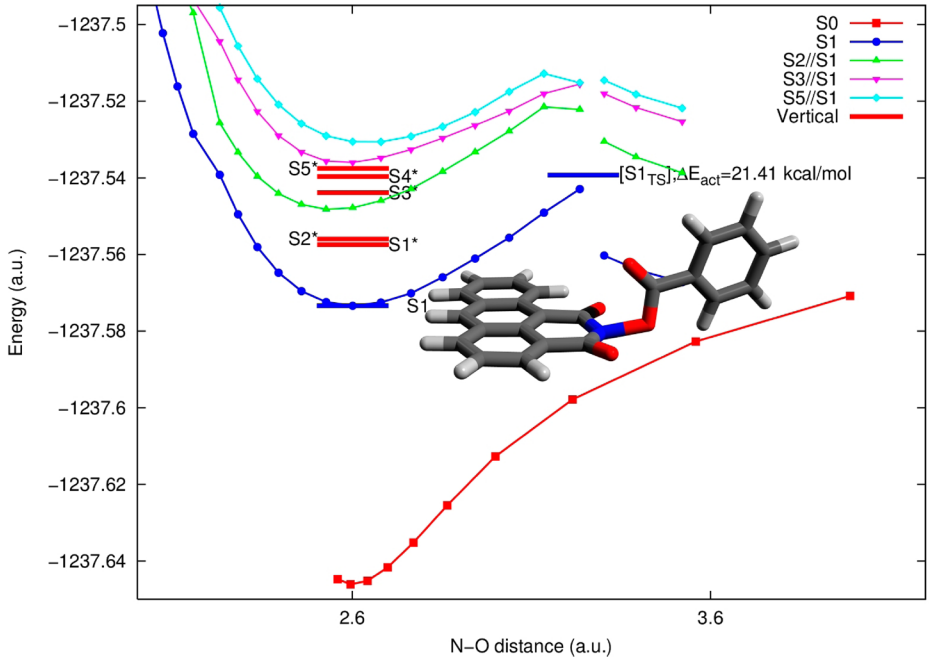

Figure 4. Potential energy surface for the dissociation of theN−O bond in **3b**. Calculations were done at the PBE/def2-SVP level of theory. The geometry of the transition state is shown.

the TD-PBE/def2-SVP level is 21.41 kcal/mol. The corresponding barriers in other functionals are 16.93 (B3LYP), 24.70 (CAM-B3LYP), 22.96 (PBE0), and 17.42 kcal/mol (TPSSh). The energies were computed at the geometries obtained from PBE/def2-SVP optimizations. In conclusion, TD-DFT calculations support the proposed mechanism of homolytic N−O bond cleavage in the lowest singlet excited state.

5. HADI-Based Polymer for Modification of Silicon Surfaces. After successfully demonstrating sulfonyloxy anthracene-1,9-dicarboxyimides as PAGs for sulfonic acids, our attention turned toward the synthesis of polymers bearing sulfonates which on photoirradiation generate sulfonic acids. Further, we wanted to use the aforementioned polymers to prepare SiO_2/polymer hybrid materials for the development of photoresponsive organosilicon surfaces.

5.1. Synthesis of the Monomer N-(p-Vinylbenzenesulfonyloxy)anthracene-1,9-dicarboxyimide (VBSADI). The schematic synthesis of the monomer VBSADI (**9**) is described in Scheme 4. Under an N_2 atmosphere *p*-vinylbenzene sulfonyl chloride[33]

Scheme 4. Synthesis of the Monomer VBSADI (9)

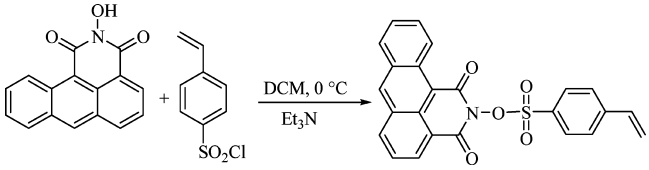

was added to HADI in dry DCM, and then Et_3N was added slowly into the reaction mixture. The reaction mixture was stirred overnight at room temperature to obtain the orange monomer VBSADI.

5.2. Synthesis of N-(p-Vinylbenzenesulfonyloxy)-anthracene-1,9-dicarboxyimide−Methyl Methacrylate (VBSADI-MMA) and N-(p-Vinylbenzenesulfonyloxy)-anthracene-1,9-dicarboxyimide−Ethyl Acrylate (VBSADI-EA) copolymers. The polymers VBSADI-MMA and VBSADI-EA were synthesized using the ATRP[34] process. The monomer VBSADI (**9**), cuprous bromide (CuBr), and ethyl 2-bromoisobutyrate (EBiB) as an initiator were mixed with dry DMF in a Schlenk flask. The solution was degassed by three freeze−pump−thaw cycles. Further, the ligand *N*,*N*,*N*′,*N*′,*N*″-pentamethyldiethylenetriamine (PMDETA) in dry DMF was injected into the reaction mixture and then heated at 40 °C for 6 h. The reaction vessel was maintained in liquid nitrogen, and DMF was removed by rotary evaporation. Finally the polymer was dissolved in THF and passed through a neutral Al_2O_3 column to remove the copper catalyst. The volume of THF was removed, and the polymer was precipitated from a hexane/methanol (1/1) mixture at 0 °C. This process was repeated three times for a complete removal of unreacted monomer. A yellow solid polymer was recovered, and its molecular weight was determined by GPC methods.

Using the same procedure as described for the synthesis of the homomer, copolymers were synthesized in dry DMF using the monomer VBSADI with ethyl acrylate (EA) and methyl methacrylate (MMA) individually, as shown in Scheme 5.

*5.3. Characterization of the Polymers VBSADI-MMA (**12**) and VBSADI-EA (**13**).* Molecular weights and polydispersities of the polymers VBSADI-MMA (**12**) and VBSADI-EA (**13**) were recorded by gel permeation chromatography (GPC) and are tabulated in Table 4. GPC (Figure 5) was carried out at ambient temperature using a Viscotek-GPC system equipped with two GMH HR-H nonpolar organic columns in series. DMF was used as an eluent, at a flow rate of 1 mL/min. Polystyrene standard in the M_n range of 2000−395000 was used for calibrations. Further, the polymers synthesized above were also characterized by UV/vis and fluorescence spectroscopy (see the Supporting Information, Figure F4a,b, p S16) and IR and ^1H NMR spectroscopy.

5.4. Photoinduced Generation of Sulfonic Acid from Polymer Film. To investigate the polymers as PAGs, the

dx.doi.org/10.1021/jo301367y | J. Org. Chem. 2012, 77, 10557−10567

Scheme 5. Synthesis of the Copolymers VBSADI-MMA (12) and VBSADI-EA (13)

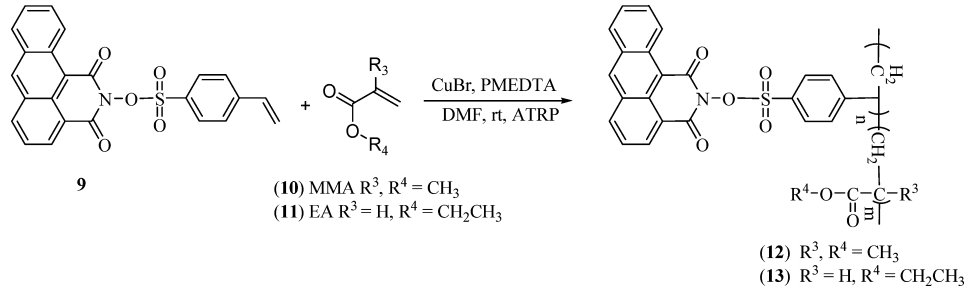

9

(**10**) MMA R^3, $R^4 = CH_3$
(**11**) EA $R^3 = H$, $R^4 = CH_2CH_3$

(**12**) R^3, $R^4 = CH_3$
(**13**) $R^3 = H$, $R^4 = CH_2CH_3$

Table 4. Polymerization Conditions and Characterization of Polymers

polymer	sample	VBSADI	MMA	EA	CuBr	PMDETA	EBiB	M_n[a]
12	VBSADI-MMA copolymer	0.07 g, 0.158 mmol	0.0158 g, 0.158 mmol		0.452 mg, 0.00316 mmol	0.819 mg, 0.00474 mmol	0.622 mg, 0.00316 mmol	2980
13	VBSADI-EA copolymer	0.07 g, 0.158 mmol		0.016 g, 0.16 mmol	0.452 mg, 0.00316 mmol	0.819 mg, 0.00474 mmol	0.622 mg, 0.00316 mmol	3140
14	homopolymer	0.07 g, 0.158 mmol			0.226 mg, 0.00158 mmol	0.273 mg, 0.00158 mmol	0.311 mg, 0.00158 mmol	2190

[a]Measured against polystyrene standards.

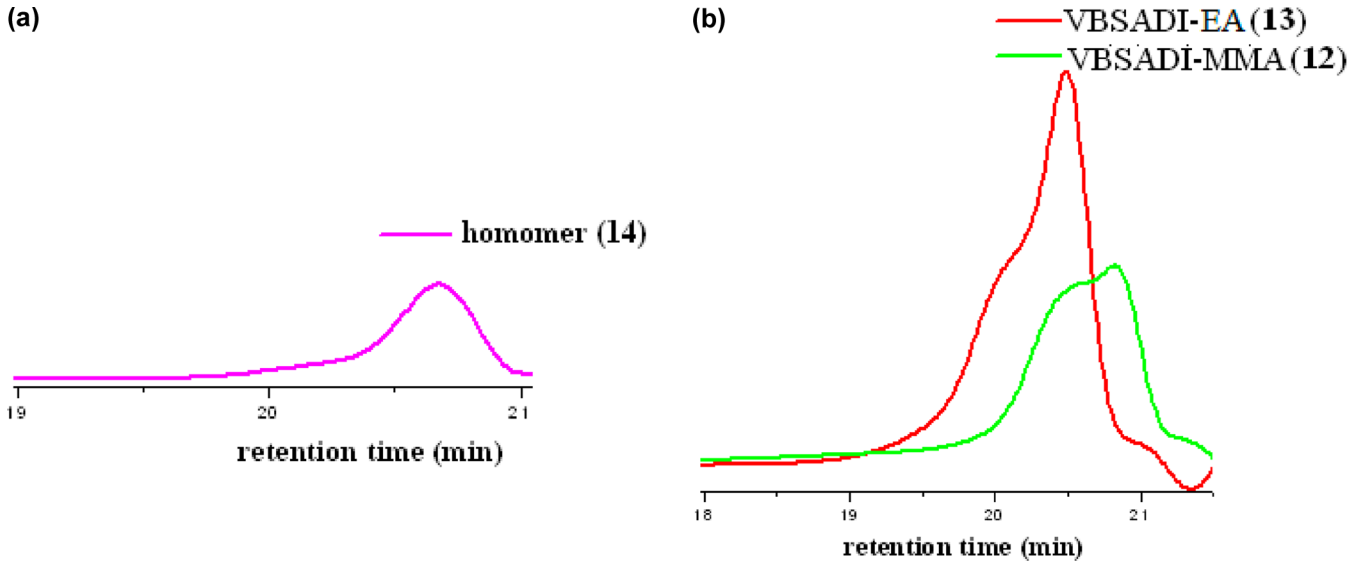

Figure 5. GPC of (a) homomer **14** and (b) copolymers VBSADI-MMA (**12**) and VBSADI-EA (**13**).

Scheme 6. Photogeneration of Sulfonic Acid from Polymer Film

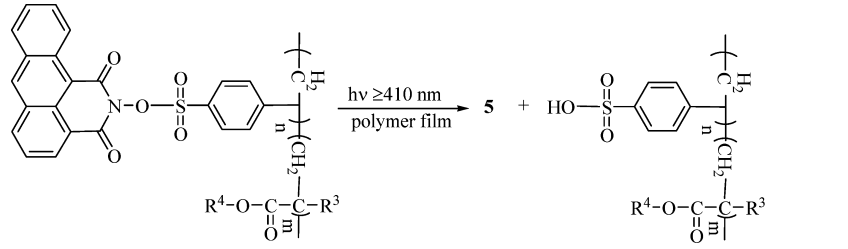

(**12**) R^3, $R_4 = CH_3$
(**13**) $R^3 = H$, $R^4 = CH_2CH_3$

(**15**) R^3, $R^4 = CH_3$
(**16**) $R^3 = H$, $R^4 = CH_2CH_3$

VBSADI-MMA (**12**) polymer was spin-coated onto a thin glass slide using a Headway Research spinner (Spin Coating Unit SCU 2005). The polymer films were then baked at 90 °C for 5 min in an oven. The film thicknesses were measured with a Dektak-150 film thickness measurement gauge. Irradiation of polymer thin films using UV light above 410 nm resulted in photodecomposition of the polymer, leading to the generation of sulfonic acid (Scheme 6).

The FT-IR spectrum (see the Supporting Information, Figure F5a, p S17) indicated photolysis of polymer films (VBSADI-MMA). Peaks at 1385, 1193, and 1180 cm^{-1} ($\nu(SO_2)$) due to aminosulfonate units decreased, indicating

dx.doi.org/10.1021/jo301367y | J. Org. Chem. 2012, 77, 10557−10567

the photodecomposition of the polymer. On the other hand, the generation of sulfonic acid by the polymer films was confirmed by using acid-catalyzed polysiloxane formation techniques.[35] FT-IR spectra (see the Supporting Information, p S17, Figure F5b) showed changes in the irradiated film before and after treatment with methyltriethoxysilane (MTEOS). The appearance of new peaks at 780 (Si−CH_3), 900 (Si−OH), 1000−1200 (Si−O−Si), and 3200−3500 cm^{-1} (Si−OH) supported the formation of silanol, which was obtained on hydrolysation of MTEOS under humid conditions by the photogenerated sulfonic acid.

6. Modification of Silicon Surfaces using VBSADI-MMA. The organosilica surface was prepared by the addition of SiO_2 to the DCM-containing polymer VBSADI-MMA, and the mixture was stirred for 1 day at room temperature. Then the mixture was collected by centrifugation (8000 rpm, 10 min). Finally a rough surface of organosilica (for corresponding FT-IR spectra of SiO_2/polymer hybrid material, see the Supporting Information, Figure F6, p S17) was obtained on the glass plate. The plate was kept in a hot oven for 2 h to remove the lagging solvent completely.

The hydrophobicity of the surface was tested by measuring the water contact angle (CA). Initially, the prepared organosilica surface exhibited a large contact angle (i.e., hydrophobic in nature in comparison to a common silica surface, which is hydrophilic). The rough structure on the coating surface and low surface energy[14,36] are believed to contribute to the hydrophobic properties of organosilica (the water droplet rolls off spontaneously for a longer time on the surface). However, the surface of organosilica loses its hydrophobicity and becomes superhydrophilic on gradual photoirradiation (≥410 nm), as shown in Figure 6. On photolysis, the polymer decomposes and generates a polar −SO_3H unit, which leads to a decrease in the contact angle (CA).

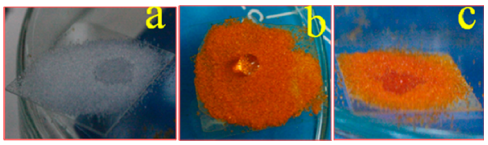

Figure 6. (a) Water drop on a common silica (60−120) surface, showing superhydrophilicity. (b) Water drop on the organosilica surface, showing large hydrophobicity. (c) Water drop on the organosilica surface after photoirradiation, behaving as a superhydrophilic surface.

The irreversible change of the modified organosilica surface from hydrophobic to hydrophilic in term of contact angle (CA) at regular time intervals of photoirradiation is shown in Figure 7.

OUTLOOK

In comparison to the well-known PAGs, our newly developed PAGs based on HADI provided certain advantages such as the following: (i) they exhibit strong fluorescence and relatively higher fluorescence quantum yield; (ii) the fluorescence properties were found to be highly sensitive to the solvent environment, thus making them an environment-ally sensitive PAGs; (iii) they generated both carboxylic and sulfonic acids in high chemical (75−85%) and quantum yields (0.29−0.35) in the visible wavelength region (≥410 nm); (iv) they are soluble in a wide range of organic solvents. Further, we also demonstrated the application of our fluorescent PAGs in the development of a smart photoresponsive organosilica surface which changes surface wettability in the presence of external light.

EXPERIMENTAL SECTION

General Considerations. The ^1H and ^{13}C spectra were recorded in $CDCl_3$/DMSO-d_6 solvents on a 200/400 MHz spectrometer using TMS as the internal standard. HRMS was measured using a TOF analyzer.

Computational Methods. We have used density functional theory (DFT) calculations using PBE[37] functional in conjunction with def2-SVP[38] basis set. In addition, empirical dispersion correction (DFT-D)[39] and resolution of the identity (RI) approximations were used. Turbomole v6.2[40] was used for all calculations. For excited-state calculations time-dependent density functional theory (TDDFT) was employed. The unrestricted formalism was used. We have included the four lowest roots for each calculation. Dl-find,[41] implemented in ChemShell,[42] was used for optimizations. In order to compute transition states at the excited state potential energy surface (PES), the dimer method[43] was used. Vibrational analysis was done using a finite-difference Hessian in ChemShell for the excited-state calculations, and analytic gradients from Turbomole were used for ground-state calculations. Single-point energy evaluations were done with the Gaussian 09 package[44] using B3LYP,[45] CAM-B3LYP,[46] PBE0,[47] and TPSSh.[48]

Synthesis of *N*-Hydroxyanthracene-1,9-dicarboximide (2). To a mixture of anthracene-1,9-dicarboxylic anhydride (1 g, 4.03 mmol) in pyridine (10 mL) was added hydroxylamine hydrochloride (272 mg, 3.91 mmol), and this mixture was heated at 100 °C for 15 h. The reaction mixture was poured into 50 mL of 1 N HCl. The precipitate was filtered and washed with water. The crude product was dried and purified by column chromatography.

*N-Hydroxyanthracene-1,9-dicarboximide (**2**).* The crude product was purified by column chromatography (20% ethyl acetate/hexane) to give the title compound **2** (890 mg, 84%) as a deep yellow solid: R_f (50% ethyl acetate/hexane) 0.35; mp 255−257 °C; FTIR (neat) ν_{max} (cm^{-1}) 3466, 1664; ^1H NMR ($CDCl_3$, 200 MHz) δ 7.69−7.95 (m, 3H), 8.18 (d, 1H, J = 8.2 Hz), 8.46 (d, 1H, J = 7.8 Hz), 8.88 (d, 1H, J = 7.2 Hz), 8.94 (s, 1H), 9.98 (d, 1H, J = 9.0 Hz); ^{13}C NMR ($CDCl_3$, 100 MHz) δ 114.1, 125.6, 126.1, 126.9, 129.8, 132.2, 133.6, 134.6, 136.3, 138.0, 157.7, 160.8: HRMS (ES^+) calcd for $C_{16}H_{10}NO_3$ [M + H^+] 264.0655, found 264.0651.

General Procedure for the Synthesis of PAGs 3a−e. To a DCM solution of *N*-hydroxyanthracene-1,9-dicarboxyimide (300 mg, 1.14 mmol) was added slowly Et_3N (2.27 mmol) while the temperature of the reaction solution was maintained at 0 °C; acid chloride which was dissolved in dry DCM was slowly added to the reaction mixture, and this mixture was stirred for a further 12 h at room temperature. After completion of the reaction cold distilled water was poured into the reaction mixture and diluted with DCM. The organic layer was separated and dried over Na_2SO_4, and the solvent was removed under vacuum to yield the orange crude carboxylate ester.

*N-(Phenylacetyloxy)anthracene-1,9-dicarboximide (**3a**).* The yellow solid compound **3a** (335 mg, 80%) was obtained by purification of the crude product using column chromatography (20% ethyl acetate/hexane): R_f (25% ethyl acetate/hexane) 0.35; mp 184−186 °C; FTIR (KBr) ν_{max} (cm^{-1}) 1683, 1708, 1799; ^1H NMR ($CDCl_3$, 200 MHz) δ 4.19 (s, 2H), 7.35−7.56 (m, 5H), 7.67−7.95 (m, 3H), 8.19 (d, 1H, J = 7.8 Hz), 8.49 (d, 1H, J = 8.2 Hz), 8.85 (d, 1H, J = 7.0 Hz), 8.97 (s,

dx.doi.org/10.1021/jo301367y | J. Org. Chem. 2012, 77, 10557−10567

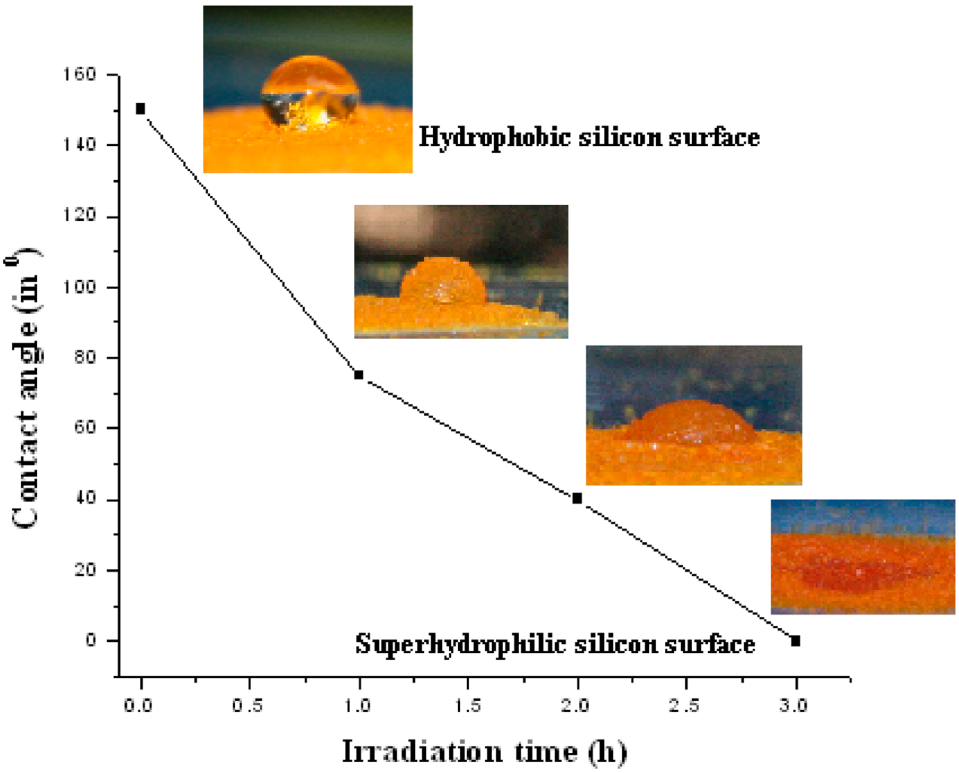

Figure 7. Variation in the contact angle of the organosilica surface with irradiation time.

1H), 9.95 (d, 1H, J = 8.8 Hz); ^{13}C NMR ($CDCl_3$, 50 MHz) δ 38.1, 114.1, 121.5, 125.2, 125.9, 126.6, 127.6, 128.5, 128.8 (3C), 129.6 (3C), 131.7, 131.9, 132.2, 133.5, 134.1, 136.2, 137.5, 158.9, 160.0, 168.0; HRMS (ES^+) calcd for $C_{26}H_{18}N_2O_4$ [M + CH_3CN] 422.1266, found 422.1262.

*N-(Benzoyloxy)anthracene-1,9-dicarboximide (**3b**).* Purification of the crude carboxylate by column chromatography (25% ethyl acetate/hexane) gives title compound **3b** (343 mg, 82%) as a yellow solid: R_f (40% ethyl acetate/hexane) 0.45; mp 208−210 °C; FTIR (KBr) ν_{max} (cm^{-1}) 1684, 1703, 1772; ^{1}H NMR ($CDCl_3$, 200 MHz) δ 7.46−7.61 (m, 2H), 7.67−7.88 (m, 4H), 8.16 (d, 1H, J = 8.6 Hz), 8.33 (d, 2H, J = 7.2 Hz), 8.46 (d, 1H, J = 8.2 Hz), 8.80 (d, 1H, J = 7.4 Hz), 8.94 (s, 1H), 9.94 (d, 1H, J = 9 Hz); ^{13}C NMR ($CDCl_3$, 50 MHz): 114.6, 122.0, 125.4, 126.2, 126.7, 127.2, 128.2, 128.7, 128.8, 128.9, 129.7, 130.5, 130.8, 131.9, 132.2, 133.9, 134.4, 134.7, 136.3, 137.6, 159.2, 160.4, 163.1; HRMS (ES^+) calcd for $C_{24}H_{15}NO_6$ [M + HCO_2H] 413.0899, found 413.0895.

*N-(p-Methylbenzoyloxy)anthracene-1,9-dicarboximide (**3c**).* The compound **3c** (347 mg, 80%) was obtained as a yellow solid on purification of the crude product through column chromatography (20% ethyl acetate/hexane): R_f (50% ethyl acetate/hexane) 0.60; mp 193−195 °C; FTIR (KBr) ν_{max} (cm^{-1}) 1678, 1701, 1773; ^{1}H NMR ($CDCl_3$, 200 MHz) δ 2.48 (s, 3H), 7.36 (d, 1H, J = 8.0 Hz), 7.64−7.89 (m, 3H), 8.15−8.23 (m, 3H), 8.47 (d, 1H, J = 8.6 Hz), 8.86 (d, 1H, J = 9.0 Hz), 8.95 (m, 1H), 9.94 (d, 1H, J = 8.6 Hz); ^{13}C NMR ($CDCl_3$, 50 MHz) δ 22.1, 114.5, 122.0, 123.6, 125.4, 126.2, 126.8, 127.1, 127.7, 128.8, 129.7, 129.9, 130.2, 130.8, 131.9, 132.2, 133.9, 134.3, 136.4, 137.7, 145.6, 159.4, 160.5, 163.4; HRMS (ES^+) calcd for $C_{24}H_{16}NO_4$ [M + H^+] 382.1074, found 382.1078.

*N-(p-Methoxybenzoyloxy)anthracene-1,9-dicarboximide (**3d**).* The dark yellow crude solid carboxylate on purification by column chromatography (30% ethyl acetate/hexane) gives the title compound **3d** (357 mg, 79%) as an orange solid: R_f (50% ethyl acetate/hexane) 0.70; mp 225−227 °C; FTIR (KBr) ν_{max} (cm^{-1}) 1676, 1702, 1762; ^{1}H NMR ($CDCl_3$, 400 MHz) δ 3.96 (brs, 3H), 7.06 (d, 2H, J = 8.8 Hz), 7.64−7.85 (m, 3H), 8.15 (d, 1H, J = 8.8 Hz), 8.31 (d, 2H, 8.8 Hz), 8.45 (d, 1H, J = 8.0 Hz), 8.81 (d, 1H, J = 8 Hz), 8.92 (s, 1H), 9.91 (d, 1H, J = 9.2 Hz); ^{13}C NMR ($CDCl_3$, 100 MHz) δ 55.5, 114.01, 114.08, 114.5, 118.3, 121.9, 125.5, 126.6, 127.0, 127.7, 128.7, 129.4, 129.7, 130.0, 131.7, 132.1, 132.2, 133.8, 134.2, 136.2, 137.5, 159.3, 160.5, 162.7, 164.5; HRMS (ES^+) calcd for $C_{26}H_{18}N_2O_5$ [M + CH_3CN] 438.1216, found 438.1211.

*N-(p-Nitrobenzoyloxy)anthracene-1,9-dicarboximide (**3e**).* Purification of the crude carboxylate by column chromatography (25% ethyl acetate/hexane) gives the title compound **3e** (352 mg, 75%) as a yellow solid: R_f (40% ethyl acetate/hexane) 0.45; mp 260−264 °C; FTIR (KBr) ν_{max} (cm^{-1}) 1684, 1699, 1774; ^{1}H NMR ($CDCl_3$, 400 MHz) δ 7.68−7.71 (m, 1H), 7.79−7.85 (m, 1H), 7.87−7.89 (m, 1H), 8.18 (d, 1H, J = 8.8 Hz), 8.44−8.50 (m, 3H), 8.53−8.88 (m, 2H), 8.84 (d, 1H, 8.84 Hz), 8.96 (s, 1H), 9.87 (d, 1H, J = 8.8 Hz); ^{13}C NMR ($CDCl_3$, 50 MHz) δ 121.5, 123.9 (2C), 125.9, 126.2, 127.0, 127.3, 128.1, 129.0, 129.9, 131.8 (2C), 132.2, 132.4, 134.2, 134.8, 136.7, 138.0, 139.3, 151.4, 159.1, 160.2, 161.6; HRMS (ES^+) calcd for $C_{23}H_{13}N_2O_6$ [M + H^+] 413.0768, found 413.0761.

General Procedure for the Synthesis of PAGs 4a−e. To a mixture of sulfonyl chloride (1.5 mmol) and *N*-hydroxyanthracene-1,9-dicarboximide (250 mg, 0.95 mmol) in dry DCM was added Et_3N (0.52 mL, 1.90 mmol) dropwise at 0 °C. The reaction mixture was then stirred overnight at room temperature. After the completion of the reaction, it was quenched by ice-cold water, diluted with DCM. The organic layer was separated and dried over Na_2SO_4, and the solvent was removed under vacuum to yield the orange crude sulfonate.

dx.doi.org/10.1021/jo301367y | J. Org. Chem. 2012, 77, 10557−10567

*N-(Methylsulfonyloxy)anthracene-1,9-dicarboximide (**4a**).* The crude product was purified by column chromatography (20% ethyl acetate/hexane) to give the title compound **4a** (265 mg, 82%) as an orange solid: R_f (40% ethyl acetate/hexane) 0.45; mp 218−220 °C; FTIR (KBr) ν_{max} (cm^{-1}) 1387, 1689, 1717; ^1H NMR (DMSO-d_6, 200 MHz) δ 3.74 (s, 3H), 7.66 (t, 1H, J = 7.2 Hz), 7.79−7.90 (m, 2H), 8.19 (d, 1H, J = 8.2 Hz), 8.55−8.67 (m, 2H), 9.14 (s, 1H), 9.59 (d, 1H, J = 9.0 Hz); ^{13}C NMR (DMSO-d_6, 50 MHz) δ 39.0, 114.2, 121.8, 125.6, 126.5, 127.4, 127.7, 129.1, 130.9, 132.3, 132.9, 133.5, 135.5, 137.7, 139.3, 159.9, 161.1; HRMS (ES^+) calcd for $C_{17}H_{12}NO_5S$ [M + H^+] 342.0431, found 342.0427.

*N-(1-Butanesulfonyloxy)anthracene-1,9-dicarboximide (**4b**).* Purification of the crude product by column chromatography (25% ethyl acetate/hexane) gives the title compound **4b** (291 mg, 80%) as a yellow solid: R_f (30% ethyl acetate/hexane) 0.50; mp 210−213 °C; FTIR (KBr) ν_{max} (cm^{-1}) 1387, 1686, 1711; ^1H NMR ($CDCl_3$, 200 MHz) δ 1.07 (t, 3H, J = 7.4 Hz), 1.51−1.62 (m, 2H), 2.18 (m, 2H), 3.79−3.87 (m, 2H), 7.66−7.93 (m, 3H), 8.17 (d, 1H, J = 8.4 Hz), 8.47 (d, 1H, J = 8.0 Hz), 8.83 (d, 1H, J = 6.2), 8.94 (s, 1H), 9.94 (d, 1H, J = 9.0 Hz); ^{13}C NMR ($CDCl_3$, 50 MHz) δ 13.7, 21.7, 25.8, 54.4, 114.2, 121.6, 125.6, 126.2, 127.0, 127.6, 128.7, 129.9, 132.2, 133.9, 134.8, 136.8, 138.1, 159.8, 160.8; HRMS (ES^+) calcd for $C_{20}H_{18}NO_5S$ [M + H^+] 384.0900, found 384.0905.

*N-(Phenylsulfonyloxy)anthracene-1,9-dicarboximide (**4c**).* The crude product on purification by column chromatography (20% ethyl acetate/hexane) yielded the title compound **4c** (287 mg, 75%) as an orange solid: R_f (50% ethyl acetate/hexane) 0.55; mp 225−227 °C; FTIR (KBr) ν_{max} (cm^{-1}) 1378, 1689; ^1H NMR ($CDCl_3$, 400 MHz) δ 7.66−7.78 (m, 3H), 7.79−7.89 (m, 2H), 7.90−7.92 (m, 1H), 8.19 (d, 1H, J = 8.4 Hz), 8.23−8.25 (m, 1H), 8.48 (d, 1H, J = 8.4 Hz), 8.81−8.83 (m, 1H), 8.96 (s, 1H), 9.86 (d, 1H, J = 8.8 Hz); ^{13}C NMR ($CDCl_3$, 50 MHz) δ 114.3, 121.6, 125.4, 126.1, 126.3, 126.8, 126.9, 128.7, 129.2 (2C), 129.5 (2C), 129.7, 132.0, 133.7, 134.7, 135.0, 135.4, 136.5, 137.8, 159.4, 160.4; HRMS (ES^+) calcd for $C_{22}H_{14}NO_5S$ [M + H^+] 404.0587, found 404.0581.

*N-(Tolylsulfonyloxy)anthracene-1,9-dicarboximide (**4d**).* The yellow solid compound **4d** (316 mg, 80%) was obtained by purification of the crude product using column chromatography (30% ethyl acetate/hexane): R_f (30% ethyl acetate/hexane) 0.50; mp 208−210 °C; FTIR (KBr) ν_{max} (cm^{-1}) 1386, 1697, 1717; ^1H NMR ($CDCl_3$, 200 MHz) δ 2.52 (s, 3H), 7.44 (d, 2H, 8.6 Hz), 7.63−7.89 (m, 3H), 8.09 (d, 2H, J = 8.4 Hz), 8.14 (d, 1H, J = 9.2 Hz), 8.44 (d, 1H, J = 8.4 Hz), 8.78 (d, 1H J = 7.2 Hz), 8.91 (s, 1H), 9.82 (d, 1H, J = 9.2 Hz); ^{13}C NMR ($CDCl_3$, 50 MHz) δ 22.0, 114.7, 122.0, 125.6, 126.4, 127.0, 127.8, 129.0, 129.7 (3C), 129.9 (3C), 130.0, 132.1, 132.5, 134.0, 136.6, 137.8, 146.5, 159.6, 160.7; HRMS (ES^+) calcd for $C_{23}H_{16}NO_5S$ [M + H^+] 418.0743, found 418.0740.

*N-(2,4-Difluorobenzenesulfonyloxy)anthracene-1,9-dicarboximide (**4e**).* The crude sulfonate was purified by column chromatography (30% ethyl acetate/hexane) to give the title compound **4e** (329 mg, 79%) as an orange solid: R_f (40% ethyl acetate/hexane) 0.45; mp 223−225 °C; FTIR (KBr) ν_{max} (cm^{-1}) 1387, 1689, 1717; ^1H NMR ($CDCl_3$, 400 MHz) δ 7.12−7.16 (m, 2H), 7.69−7.73 (m, 1H), 7.79 (t, 1H, J = 7.6 Hz), 7.87−7.91 (m, 1H), 7.97−8.03 (m, 1H), 8.18 (d, 1H, J = 8.4 Hz), 8.48 (d, 1H, J = 8.4 Hz), 8.78 (d, 1H, J = 7.2 Hz), 8.96 (s, 1H), 9.80 (d, 1H, J = 9.2 Hz); ^{13}C NMR ($CDCl_3$, 100 MHz) δ 106.2, 112.1, 114.0, 121.7, 123.5, 125.4, 126.2, 127.0, 128.9, 129.7, 132.2, 132.3, 132.8, 132.9, 134.1, 134.8, 136.6, 137.9, 159.3, 160.3; HRMS (ES^+) calcd for $C_{22}H_{12}F_2NO_5S$ [M + H^+] 440.0399, found 440.0390.

General Procedure for the Synthesis of the Monomer *N*-(*p*-Vinylbenzenesulfonyloxy)anthracene-1,9-dicarboximide (9). To a mixture of *N*-hydroxyanthracene-1,9-carboxyimide (500 mg, 1.90 mmol) and 4-styrenesulfonyl chloride (2.84 mmol) in dry DCM was added Et_3N (0.52 mL, 3.80 mmol) dropwise at 0 °C. The reaction mixture was then stirred overnight at room temperature. After the completion of the reaction, it was quenched by ice-cold water, diluted with DCM. The organic layer was separated and dried over Na_2SO_4, and the solvent was removed under vacuum to yield the orange crude monomer.

*N-(p-Vinylbenzenesulfonyloxy)anthracene-1,9-dicarboximide (**9**).* The crude product was purified by column chromatography (30% ethyl acetate/hexane) to give the title compound **9** (676 mg, 83%) as a deep orange solid: mp 195−198 °C; R_f (30% ethyl acetate/hexane) 0.40; FTIR (KBr) ν_{max} (cm^{-1}) 1386, 1717, 1734; ^1H NMR ($CDCl_3$, 200 MHz) δ 5.53 (d, 1H, J = 10.8 Hz), 5.98 (d, 1H, J = 17.6 Hz), 6.82 (dd, 1H, J_1 = 11.2 Hz, J_2 = 17.8 Hz), 7.62−7.71 (m, 3H), 7.73−7.89 (m, 2H), 8.13−8.17 (m, 3H), 8.45 (d, 1H, J = 8.4 Hz), 8.79 (d, 1H, J = 7.0 Hz), 8.92 (s, 1H), 9.81 (d, 1H, J = 9.0 Hz); ^{13}C NMR ($CDCl_3$, 100 MHz) δ 114.4, 118.5, 121.7, 125.3, 126.1, 126.6, 126.8, 127.6 (2C), 128.7, 129.6, 129.8 (2C), 131.9, 132.1, 133.8, 133.9, 134.6, 135.2, 136.3, 137.6, 144.0, 159.3, 160.4; HRMS (ES^+) calcd for $C_{24}H_{16}NO_5S$ [M + H^+] 430.0743, found 430.0740.

Photophysical Poperties of PAGs 3a−e and 4a−e. The UV/vis absorption spectra of degassed 1.5×10^{-5} M solutions of the PAGs **3a−e** and **4a−e** in absolute ethanol were recorded on a Shimadzu UV-2450 UV/vis spectrophotometer, and the fluorescence emission spectra were recorded on a Hitachi F-7000 fluorescence spectrophotometer. The fluorescence quantum yields of the PAGs were calculated using eq 1,[49]

$$(\Phi_f)_{PAG} = (\Phi_f)_{ST} \frac{(Grad_{PAG})}{(Grad_{ST})} \frac{\eta^2_{PAG}}{\eta^2_{ST}} \quad (1)$$

where the subscripts PAG and ST denote the photoacid generator and standard, respectively. Quinine sulfate in ethanol was taken as a standard. Φ_f is the fluorescence quantum yield; Grad is the gradient from the plot of integrated fluorescence intensity vs absorbance, and η is the refractive index of the solvent.

Since the fluorescences for photoacid generators and standard were recorded in the same solvent, eq 1a was used for the calculation of fluorescence quantum yield.

$$(\Phi_f)_{PAG} = (\Phi_f)_{ST} \frac{Grad_{PAG}}{Grad_{ST}} \quad (1a)$$

Preparative Photolysis of PAGs 3a−e and 4a−e. Nitrogen-purged solutions of PAGs **3a−e** and **4a−e** (0.05 mmol) in acetonitrile were irradiated individually under visible light (≥410 nm). The photoreaction was monitored by TLC at regular intervals. After completion of photolysis, solvent was removed under vacuum and the photoproducts anthracene-1,9-dicarboxyimide and the corresponding carboxylic acid or sulfonic acid were isolated by column chromatography using EtOAc in hexane as an eluant.

*Photoproduct Anthracene-1,9-dicarboxyimide (**5**):*[25b] orange solid; ^1H NMR ($CDCl_3$, 400 MHz) δ 7.67 (t, 1H, J = 7.6

dx.doi.org/10.1021/jo301367y | J. Org. Chem. 2012, 77, 10557−10567

Hz), 7.77 (t, 1H, J = 7.2 Hz), 7.87 (t, 1H, J = 8.0 Hz), 8.15 (d, 1H, 8.0 Hz), 8.43 (d, 1H, J = 8.4 Hz), 8.62 (s, 1H), 8.77 (d, 1H, J = 6.8 Hz), 8.91 (s, 1H), 9.99 (d, 1H, J = 9.2 Hz).

Further, the quantum yield for the photolysis of PAGs was calculated using eq 2

$$(\Phi_p)_{PAG} = \frac{(K_p)_{PAG}}{I_0(F_{PAG})} \quad (2)$$

Where, the subscript 'PAG' denotes photoacid generator. Φ_p is the photolysis quantum yield, k_p is the photolysis rate constant and I_0 is the incident photon flux and F is the fraction of light absorbed. Potassium ferrioxalate was used as an actinometer.

General Procedure for the Synthesis of Copolymers. The monomer *N*-(*p*-vinylbenzenesulfonyloxy)anthracene-1,9-dicarboxyimide (VBSADI, **9**; 0.07 g, 0.158 mmol), MMA or EA (0.16 mmol), CuBr (0.226 mg, 0.00158 mmol), and the initiator EBiB (0.311 mg, 0.00158 mmol) were mixed with dry DMF in a Schlenk flask, and the solutions were degassed by three freeze−pump−thaw cycles. Finally, the nitrogen-purged ligand PMDETA (0.273 mg, 0.00158 mmol) in dry DMF was injected into the reaction mixture and the postreaction mixture was heated at 40 °C for 6 h. Then the reaction vessel was immerged in liquid nitrogen, and DMF was removed by rotary evaporation. Finally the polymer was dissolved in THF and passed through a neutral Al_2O_3 column to remove the copper catalyst. The volume of THF was reduced, and the polymer was precipitated from a hexane/methanol (1/1) mixture at 0 °C. This process was repeated three times for complete removal of unreacted monomer, and finally the yellow solid polymer was found and the molecular weight of the polymer was determined by GPC.

Preparation of Modified Silicon Surfaces. A 200 g portion of SiO_2 was mixed with 30 mL of DCM containing the polymer VBSADI-MMA, and the mixture was stirred for 1 day at room temperature. Then the mixture was collected by centrifugation (8000 rpm, 10 min). Finally, an organosilica surface was obtained on a glass plate. The plate was kept in a hot oven for 2 h to remove the lagging solvent completely.

■ ASSOCIATED CONTENT

Ⓢ Supporting Information

Figures and tables giving characterization data (^{1}H and ^{13}C NMR and TOF-MS data) of *N*-hydroxyanthracene-1,9-dicarboxyimide based PAGs **3a−e** and **4a−e**, monomer **9**, and copolymers **12** and **13** and computational data for N−O bond cleavage for PAG **3b**. This material is available free of charge via the Internet at http://pubs.acs.org.

■ AUTHOR INFORMATION

Corresponding Author

*E-mail: ndpradeep@yahoo.co.in (N.D.P.S.); anoop@chem.iitkgp.ernet.in (A.A.); dibakar@chem.iitkgp.ernet.in (D.D.). Tel: (+) 91-3222-282324. Fax: (+) 91-3222-282252.

Notes

The authors declare no competing financial interest.

■ ACKNOWLEDGMENTS

We thank the DST (SERC Fast Track Scheme) for financial support and the DST-FIST for the 400 MHz NMR. M.I. is grateful to the CSIR (India); R.B. and S.A. are grateful to the UGC (India) for their research fellowships.

■ REFERENCES

(1) (a) Yamato, H.; Asakura, T.; Nishimae, Y.; Matsumoto, A.; Tanabe, J.; Birbaum, J.-Luc; Murer, P.; Hintermann, T.; Ohwa, T. *J. Photopolym. Sci. Technol.* **2007**, *20*, 637. (b) Yi, Y.; Ayothi, R.; Ober, C. K.; Yueh, W.; Cao, H. *Proc. SPIE* **2008**, *6923*, 69231B−1.

(2) (a) Ayothi, R.; Yi, Y.; Cao, H. B.; Yueh, W.; Putna, S.; Ober, C. K. *Chem. Mater.* **2007**, *19*, 1434. (b) Innocenzi, P.; Kidchob, T.; Falcaro, P.; Takahashi, M. *Chem. Mater.* **2008**, *20*, 607. (c) Reichmanis, E.; Houlihan, F. M.; Nalamasu, O.; Neenan, T. X. *Chem. Mater.* **1991**, *3*, 394.

(3) (a) Torres, J. M.; Stafford, C. M.; Vogt, B. D. *Soft Matter* **2012**, *8*, 5225. (b) Koo, H. Y.; Lee, H. J.; Kim, J. K.; Choi, W. S. *J. Mater. Chem.* **2010**, *20*, 3932. (c) Arnold, P. A.; Fratesi, L. E.; Bejan, E.; Cameron, J.; Pohlers, G.; Liu, H; Scaiano, J. C. *Photochem. Photobiol. Sci* . **2004**, *3*, 864.

(4) Ito, H. *Adv. Polym. Sci.* **2005**, *172*, 37.

(5) (a) Cao, D.; Hu, M.; Han, C.; Yu, J.; Cui, L.; Liu, Y.; Cai, Y.; Wang, H.; Kang, Y. *Analyst* **2011**, *136*, 2225. (b) Wang, M.; Lee, C. T.; Henderson, C. L.; Yueh, W.; Roberts, J. M.; Gonsalves, K. E. *J. Mater. Chem.* **2008**, *18*, 2704. (c) Kim, Y. J.; Kang, H.; Leolukman, M.; Nealey, P. F.; Gopalan, P. *Chem. Mater.* **2009**, *21*, 3030. (d) Wang, M.; Gonsalves, K. E.; Rabinovich, M.; Yueh, W.; Roberts, J. M. *J. Mater. Chem.* **2007**, *17*, 1699.

(6) Steidl, L.; Jhaveri, S. J.; Ayothi, R.; Sha, J.; McMullen, J. D.; Ng, S. Y. C.; Zipfel, W. R.; Zentel, R.; Ober, C. K. *J. Mater. Chem.* **2009**, *19*, 505.

(7) (a) Shirai, M.; Okamura, H. *Prog. Org. Coat.* **2009**, *64*, 175. (b) Shirai, M. *J. Photopolym. Sci. Technol.* **2007**, *20*, 615.

(8) Aveline, B. M.; Kochever, I. E.; Redmond, R. W. *J. Am. Chem. Soc.* **1995**, *117*, 9699.

(9) Ikbal, M.; Banerjee, R.; Atta, S.; Jana, A.; Dhara, D.; Anoop, A.; Singh, N. D. P. *Chem. Eur. J.* **2012**, *18*, 11968.

(10) Xu, W.; Li, T.; Li, G.; Wu, Y.; Miyashita, T. *J. Photochem. Photobiol. A: Chem.* **2011**, *219*, 50.

(11) (a) Li, C.; Cheng, F.; Lv, J.; Zhao, Y.; Liu, M.; Jiang, L.; Yu, Y. *Soft Matter* **2012**, *8*, 3730. (b) Pasparakis, G.; Vamvakaki, M. *Polym. Chem.* **2011**, *2*, 1234. (c) Wang, S.; Song, Y.; Jiang, L. *J. Photochem. Photobiol. C: Photochem. Rev.* **2007**, *8*, 18. (d) Stegmaier, P.; Alonso, J. M.; Campo, A. d. *Langmuir* **2008**, *24*, 11872.

(12) (a) Kamegawa, T.; Sakai, T.; Matsuoka, M.; Anpo, M. *J. Am. Chem. Soc.* **2005**, *127*, 16784. (b) Cazacu, M.; Dragan, S.; Vlad, A. *J. Appl. Polym. Sci.* **2003**, *88*, 2060. (c) Ogoshi, T.; Chujo, Y. *Comp. Interfaces* **2005**, *11*, 539. (d) Hoffmann, F.; Cornelius, M.; Morell, J.; Froba, M. *Angew. Chem., Int. Ed.* **2006**, *45*, 3216.

(13) Liu, R.; Shi, Y.; Wan, Y.; Meng, Y.; Zhang, F.; Gu, D.; Chen, Z.; Tu, B.; Zhao, D. *J. Am. Chem. Soc.* **2006**, *128*, 11652.

(14) Zhang, X.; Shi, F.; Niu, J.; Jiang, Y.; Wang, Z. *J. Mater. Chem.* **2008**, *18*, 621.

(15) (a) Shopsowitz, K. E.; Hamad, W. Y.; Maclachlan, M. J. *J. Am. Chem. Soc.* **2012**, *134*, 867. (b) Mizoshita, N.; Yamanaka, K.; Hiroto, S.; Shinokubo, H.; Tani, T.; Inagaki, S. *Langmuir* **2012**, *28*, 3987. (c) Jaroniec, M. *Nature* **2006**, *442*, 638.

(16) Budzewski, B.; Jezierska, M.; Welniak, M.; Berek, D. *J. High Res. Chromatogr.* **1998**, *21*, 267.

(17) Taguchi, A.; Schuth, F. *Microporous Mesoporous Mater.* **2005**, *77*, 1.

(18) (a) Kickelbick, G. *Prog. Polym. Sci.* **2003**, *28*, 83. (b) Merkel, T. C.; Freeman, B. D.; Spontak, R. J.; He, Z.; Pinnau, I.; Meakin, P.; Hill, A. J. *Science* **2002**, *296*, 519.

(19) Sheng, C.; Benlan, L.; Yu, L.; Xiaodong, S.; Xueyong, L.; Guifan, H. *J. Wuhan Univ. Tech. Mater. Sci. Ed.* **2011**, *26*, 1079.

(20) Xu, D.; Wang, M.; Ge, X.; Lam, M. H. W.; Ge, X. *J. Mater. Chem.* **2012**, *22*, 5784.

(21) Ikbal, M.; Jana, A.; Singh, N. D. P.; Banerjee, R.; Dhara, D. *Tetrahedron* **2011**, *67*, 3733.

(22) Chem, K. H.; Park, I. J.; Choi, M. H. *Bull. Korean Chem. Soc.* **1993**, *14*, 614.

(23) Malval, J. P.; Suzuki, S.; Savary, F. M.; Allonas, X.; Fouassier, J. P.; Takahara, S.; Yamaoka, T. *J. Phys. Chem. A* **2008**, *112*, 3879.

(24) Feng, N.; Zhao, H.; Tian, D.; Li, H. *Org. Lett.* **2012**, *14*, 1958.
(25) (a) Yao, J. H.; Chi, C.; Wu, J.; Loh, K. P. *Chem. Eur. J.* **2009**, *15*, 9299. (b) Langhals, H.; Schonmann, G.; Polborn, K. *Chem. Eur. J.* **2008**, *14*, 5290.
(26) (a) Endo, T.; Suzuki, S.; Miyagawa, N.; Takahara, S. *J. Photochem. Photobiol. A: Chem.* **2008**, *200*, 181. (b) Iwashima, C.; Imai, G.; Okamura, H.; Tsunooka, M.; Shirai, M. *J. Photopolym. Sci. Technol.* **2003**, *16*, 91.
(27) Yin, J.; Zhang, K.; Jiao, C.; Li, J.; Chi, C.; Wu, J. *Tetrahedron Lett.* **2010**, *15*, 6313.
(28) Reichardt, C. *Chem. Rev.* **1994**, *94*, 2319.
(29) Manning, S. J.; Bogen, W.; Kelly, L. A. *J. Org. Chem.* **2011**, *76*, 6007.
(30) Meech, S. R.; Phillips, D. *J. Photochem.* **1983**, *23*, 193.
(31) Connolly, J. S.; Meyer, T. H. *Photochem. Photobiol.* **1981**, *34*, 145.
(32) Ortica, F.; Scaiano, J. C.; Pohlers, G.; Cameron, J. F.; Zampini, A. *Chem. Mater.* **2000**, *12*, 414.
(33) Berrisford, D. J.; Lovell, P. A.; Suliman, N. R.; Whiting, A. *Chem. Commun.* **2005**, 5904.
(34) Tsarevsky, N. V.; Matyjaszewski, K. *Chem. Rev.* **2007**, *107*, 2270.
(35) Shinozuka, T.; Shirai, M.; Tsunooka, M. *Eur. Polym. J.* **2001**, *37*, 1625.
(36) Feng, L.; Zhang, Z.; Mai, Z.; Ma, Y.; Liu, B.; Jiang, L.; Zhu, D. *Angew. Chem., Int. Ed.* **2004**, *43*, 2012.
(37) (a) Perdew, J. P.; Burke, K.; Ernzerhof, M. *Phys. Rev. Lett.* **1996**, *77*, 3865. (b) Perdew, J. P.; Burke, K.; Ernzerhof, M. *Phys. Rev. Lett.* **1997**, *78*, 1396.
(38) (a) Eichkorn, K.; Treutler, O.; Öhm, H.; Häser, M.; Ahlrichs, R. *Chem. Phys. Lett.* **1995**, *240*, 283. (b) Eichkorn, K.; Treutler, O.; Öhm, H.; Häser, M.; Ahlrichs, R. *Chem. Phys. Lett.* **1995**, *242*, 652.
(39) Grimme, S.; Antony, J.; Schwabe, T.; Mück-Lichtenfeld, C. *Org. Biomol. Chem.* **2007**, *5*, 741.
(40) TURBOMOLE V6.2 2011, a development of University of Karlsruhe and Forschungszentrum Karlsruhe GmbH, 1989−2007, TURBOMOLE GmbH, since 2007; available from http://www.turbomole.com.
(41) Kästner, J.; Carr, J. M.; Keal, T. W.; Thiel, W.; Wander, A.; Sherwood, P. *J. Phys. Chem. A* **2009**, *113*, 11856.
(42) ChemShell, a computational chemistry shell; see www.chemshell.org.
(43) Henkelman, G.; Jónsson, H. *J. Chem. Phys.* **1999**, *111*, 7010.
(44) Frisch, M. J.; Trucks, G. W.; Schlegel, H. B.; Scuseria, G. E.; Robb, M. A.; Cheeseman, J. R.; Scalmani, G.; Barone, V.; Mennucci, B.; Petersson, G. A.; Nakatsuji, H.; Caricato, M.; Li, X.; Hratchian, H. P.; Izmaylov, A. F.; Bloino, J.; Zheng, G.; Sonnenberg, J. L.; Hada, M.; Ehara, M.; Toyota, K.; Fukuda, R.; Hasegawa, J.; Ishida, M.; Nakajima, T.; Honda, Y.; Kitao, O.; Nakai, H.; Vreven, T.; Montgomery, J. A., Jr.; Peralta, J. E.; Ogliaro, F.; Bearpark, M.; Heyd, J. J.; Brothers, E.; Kudin, K. N.; Staroverov, V. N.; Kobayashi, R.; Normand, J.; Raghavachari, K.; Rendell, A.; Burant, J. C.; Iyengar, S. S.; Tomasi, J.; Cossi, M.; Rega, N.; Millam, J. M.; Klene, M.; Knox, J. E.; Cross, J. B.; Bakken, V.; Adamo, C.; Jaramillo, J.; Gomperts, R.; Stratmann, R. E.; Yazyev, O.; Austin, A. J.; Cammi, R.; Pomelli, C.; Ochterski, J. W.; Martin, R. L.; Morokuma, K.; Zakrzewski, V. G.; Voth, G. A.; Salvador, P.; Dannenberg, J. J.; Dapprich, S.; Daniels, A. D.; Farkas, Ö.; Foresman, J. B.; Ortiz, J. V.; Cioslowski, J.; Fox, D. J. *Gaussian 09, Revision A.1*; Gaussian, Inc., Wallingford, CT, 2009.
(45) (a) Lee, C.; Yang, W.; Parr, R. G. *Phys. Rev. B* **1988**, *37*, 785. (b) Becke, A. D. *J. Chem. Phys.* **1993**, *98*, 5648.
(46) Yanai, T.; Tew, D. P.; Handy, N. C. *Chem. Phys. Lett.* **2004**, *393*, 51.
(47) Adamo, C.; Barone, V. J. *Chem. Phys.* **1999**, *110*, 6158.
(48) Staroverov, V. N.; Scuseria, G. E.; Tao, J.; Perdew, J. P. *J. Chem. Phys.* **2003**, 119.
(49) Demas, J. N.; Crosby, G. A. *J. Phys. Chem.* **1971**, *75*, 991.